

Journal of
Mechanics of
Materials and Structures

**BISTABLE STRUCTURES FOR ENERGY ABSORPTION
II. COMPOSITE STRUCTURES UNDER TENSION**

Zachary Whitman and Valeria La Saponara

Volume 2, N° 2

February 2007



mathematical sciences publishers

BISTABLE STRUCTURES FOR ENERGY ABSORPTION II. COMPOSITE STRUCTURES UNDER TENSION

ZACHARY WHITMAN AND VALERIA LA SAPONARA

This paper discusses proof-of-concept experiments of composite bistable structures and is preceded by a companion paper about metallic bistable structures. A bistable structure is characterized by a stress/strain curve with stable branches separated by unstable branches. We were interested in a particular bistable structure: one that, once activated, has a second stronger state with the ability to sustain higher loads. This allows for a better distribution of damage, and in addition the structure keeps its integrity for a longer time. Positive results on metallic configurations under tensile loading have prompted us to try and identify an equivalent composite configuration, able to show directional control of damage through this material-driven mechanism. Chain-like configurations with different reinforcements (T-300 carbon fibers, Kevlar® 49, E-glass and Dyneema®), polyurethane foam core and Kevlar stitching were conceived, designed, fabricated and investigated. Dyneema prototypes turned out to exhibit the desired bistable behavior as well as higher energy absorption than their baselines.

1. Introduction

Composites are typically characterized by high strength-to-weight and high stiffness-to-weight ratios, resistance to corrosion, and low magnetic signature. They can be tailored for a specific application. However, they are quite susceptible to delamination due to impact loading, for example, and a reduced load-carrying capacity may arise as a consequence of the impact event. Also, their brittleness is not attractive for applications where ductility, redundancy and high energy absorption are required, as in civil engineering.

Bistable structures for energy absorption were introduced by [Cherkaev and Slepyan 1995]. As discussed in the companion paper [Whitman and La Saponara 2007], the authors were asked to produce a proof-of-concept of these structures. Chain-like configurations were designed, manufactured and tested in tension. They behaved in a bistable manner, had higher energy absorption than the corresponding baselines, and a controlled type of failure. These results were obtained using metals such as 5052-H32 aluminum, C10100 copper and A36 steel.

The concepts of *main link*, *waiting link*, *percent wait* were also discussed, and will be repeated here for clarity sake. The *main link* is the part of the structure which is designed to break first. As it does, the structure does not lose its integrity because of the attached *waiting link*, which provides a redundant load path. The waiting link becomes active when the attached main link breaks. The interaction of main link and waiting link can be tuned so that the structure has the desired behavior. The *percent wait* is

Keywords: composite, energy absorption, bistable, Dyneema.

This paper is based upon work supported by the Army Research Office (grant ARO No. 41363-MA) and the National Science Foundation (grant CMMI-0621696, formerly CMS-0409514). Any opinions, findings, and conclusions or recommendations expressed in this material are those of the authors and do not necessarily reflect the views of the National Science Foundation.

the percent difference in waiting link length with respect to the attached main link length. It should be equal to the elongation to failure of the main link, however, the nonlinear behavior of the waiting link shows that this is not the case, and further tune-up of the percent wait is required for this material-driven mechanism to work.

Here we investigate structural configurations made with composite materials. The goal is, once again, to have a progressive failure where parts of the structure become active after a trigger damage event has occurred, and the damaged structure can carry a higher load with respect to its undamaged state and, more importantly, absorb more energy than its baseline. To the best of our knowledge, this study is novel.

2. Design and manufacturing

A variety of geometric configurations and percent waits was designed and manufactured with a waiting link that tried to mimic the curved waiting link present in the metallic configurations [Whitman and La Saponara 2007]. There were twenty-one iterations of this process (Table 1): nine had 12×12 plain weave¹ T300 carbon from Toray Industries Inc., four used E-glass 7715 unidirectional cloth, three had a 17×17 satin Kevlar® 49 type 285 weave, and five utilized a 10×10 satin weave made with Dyneema®, a polyethylene fiber donated by DSM Corporation. Figure 1 shows the four materials tested, Figure 2 three of the geometries used (‘small round core’, ‘medium round core’ and ‘large round core’).

The weight and thickness of the fabrics are given in Table 2. The first three fabrics have almost the same thickness, and Dyneema is almost twice as thick — as mentioned, this material was donated. Note, however, that Dyneema’s weight is very similar to T300 carbon’s, so one may extrapolate a comparison of specific energy absorptions.

Each ‘chain’ has three elements. This number was chosen because the metallic 5052-H32 aluminum bistable chains with three elements had a consistent increase in energy absorption of about 30% with respect to the baseline, and three elements were adopted as starting point of the research on composite bistable structures [Whitman and La Saponara 2007].

In addition to the reinforcement fabrics mentioned above, the following materials were used:

- (a) Last-a-Foam 6704 core, with density 64 kg/m^3 (4 lbs/ft^3). This is a closed cell polyurethane foam which is quite easy to cut (with a knife — not with hot wire, which will melt the foam), shape and machine (see Figure 3).
- (b) Kevlar 29 thread. As a main link break, the entire structure is subject to a shock. To reduce the chances of delamination, stitching was deemed necessary. The Kevlar 29 has shown to have the appropriate strength for the job, while being flexible enough to go through parts of the Consew sewing machine available.

The manufacturing process is similar for all configurations, and will be discussed here, with the aid of pictures representing one of the fabrics, Dyneema. A 152 mm wide \times 406 mm long piece of fabric was cut, which is the minimum size that guarantees three elements. Most iterations required two plies for the waiting link and one for the main link (Table 1). The size of the cuts also fit in the 355 mm diameter quilting hoop required to hold the bottom ply (for the main link) tight, and to ensure that the plies forming

¹ 12×12 means that there are 12 bundles in the warp direction and 12 bundles in the fill direction.

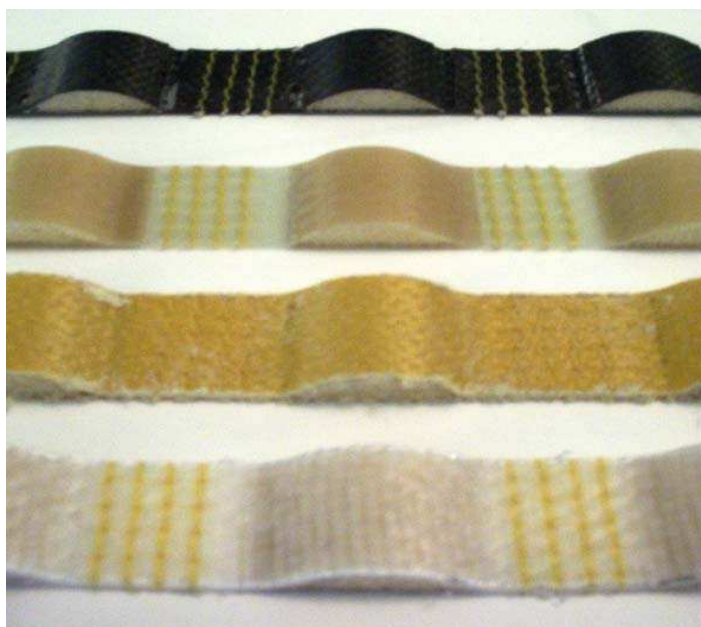


Figure 1. The four materials used: from top to bottom, T300, E-Glass, Kevlar 49, Dyneema. The width of all specimens is 25.4 mm.

the waiting link had the planned 0/90 orientation. The foam core was cut and sanded to the desired shape. In most iterations, it was found that wrapping the foam in Teflon®-coated fiberglass would help. Finally, engineering paper and plain paper were used for the stitching process, respectively to use as ‘cross-hairs’, and to protect the bottom part of the fabric during the stitching process (Figures 4 and 5). Figures 6 and 7 show additional steps of the stitching process and the specimen ready for infiltration.

The specimen was infiltrated with Epon™ 862 epoxy and EpiKure™ 9553 hardener combined at a ratio of 100:17, through vacuum-assisted resin transfer molding, a low cost, out-of-autoclave process where the vacuum pressure differential forces the resin through the specimen (Figure 8). Curing is continued for two hours in an oven at 37° C.

Each element (composed of main link and waiting link) was 50 mm in length, and each chain-like specimen had three such elements. The material forming the node (section of the specimen with four stitched rows) was ignored for this study. Its effect will be considered for future work. Because of this, the baseline specimens had length equal to 150 mm. Tabs were applied to the specimen, which was cut into samples with width equal to 25 mm. These were then tested in tension in a 222 kN screw-driven machine at a rate of 1.5 mm/minute (Figure 9).

3. Testing and discussion of results

Tables 3 and 4 show test results for the baseline specimens and for all the iterations.

The specimens of the first thirteen iterations were tested with and without the core. The core was removed (scraped out from the side of the specimen) after the cure to study its effect on the specimen’s behavior. It was assumed that the core would be compressed by the waiting link’s straightening, and

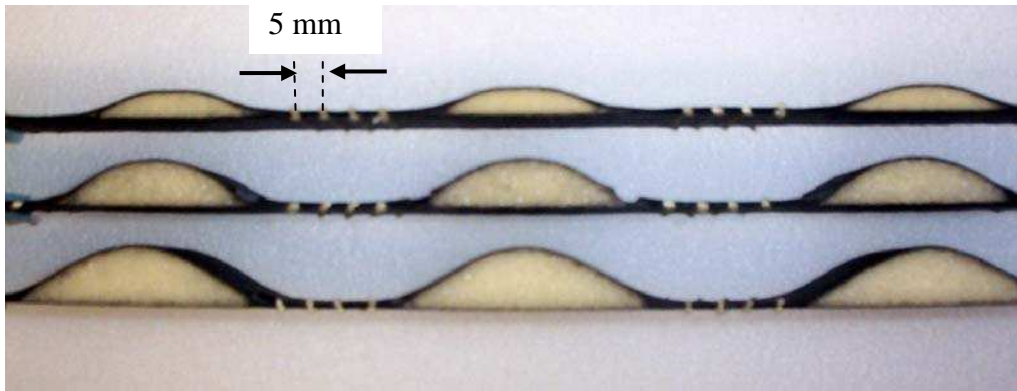


Figure 2. Three of the geometries used in this study, applied to the carbon T300 specimens: from top to bottom, specimens with small round core, medium round core and large round core. The stitch rows are 5 mm apart in all specimens.

<i>Material</i>	<i>Core shape</i>	<i>Material</i>	<i>Core shape</i>	<i>Material</i>	<i>Core shape</i>
1 T300 carbon	trapezoid	8 T300 carbon	round gumdrop	15 Kevlar	medium round
2 T300 carbon	small round	9 E-glass	trapezoid	16 Kevlar	large round
3 T300 carbon	large round	10 E-glass	small round	17 Dyneema	small round
4 T300 carbon	large round	11 E-glass	large round	18 Dyneema	medium round
5 T300 carbon	small round	12 E-glass	medium round	19 Dyneema	large round
6 T300 carbon	small round	13 T300 carbon	medium round	20 Dyneema	very large round
7 T300 carbon	large round	14 Kevlar	small round	21 Dyneema	super-large round

Table 1. Iterations of materials and configurations for this work. Only iterations 1–5 did not have the core wrapped by Teflon-coated fiberglass. Only iterations 1–3 had two plies in the main links and four plies in the waiting links. All other iterations have one ply for the main links, two plies for the waiting links.

<i>Material</i>	<i>Weight, g/m² (oz/yd²)</i>	<i>Thickness, mm (in)</i>
12 × 12 T300 carbon plain weave	271 (8)	0.23 (0.009)
E-glass 7715 unidirectional cloth	246 (7.25)	0.23 (0.009)
17 × 17 satin Kevlar 49 weave	170 (5.0)	0.25 (0.010)
10 × 10 satin Dyneema weave	264 (7.8)	0.48 (0.019)

Table 2. Material information.

that it would push the main link out of plane, thus causing premature failure. Removing the core gave mixed results: in some cases, the specimen was damaged, in others the energy absorption grew with core removal; sometimes, the load/displacement curve was bistable, but in other cases, this did not happen. This inconsistency made us decide to stop the core removal for the last eight iterations.

Among the specimens, the percent wait varied from as little as 3.9% (iteration 2) to as high as 34% (iteration 21). The number of specimens per configuration varied between two (one with core, one without) to three (with core), depending on the success of the configuration. While such numbers of specimens may not give statistically significant results, we feel that this paper addresses a wide variety of different issues, and the paper gives qualitative results that may be indicative of the general performance of the structures.

Table 5 illustrates the energies of the round core configurations (small round, medium round and large round for the four materials, plus additional iterations for the Dyneema). These are given in terms of the baselines. Dyneema was the only material that exhibited consistent higher energy absorption with respect to its baseline, as will be discussed later in this paper. The E-glass and the Dyneema were the only materials where the damaged state was stronger than the undamaged state, as indicated by bold numbers in Table 5.

In the T300, Kevlar and E-glass cases, it is easy to extrapolate that the energy associated to the bistable specimens, calculated as the area under the curve, is significantly less than for the baselines (the numbers

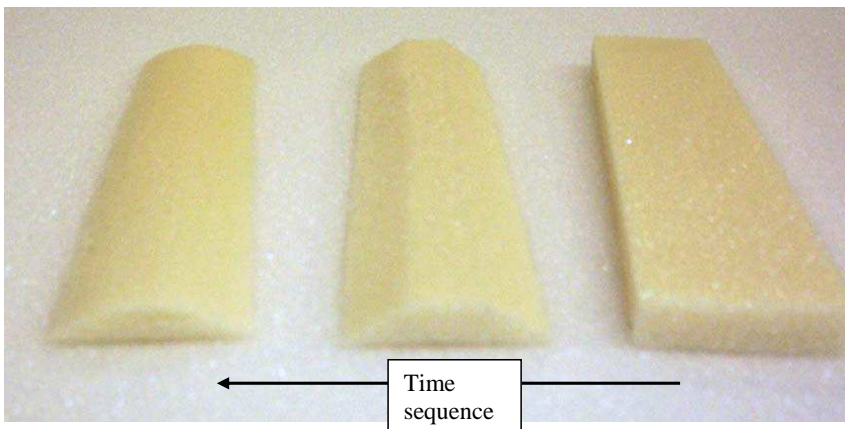


Figure 3. Steps in the process of shaping the foam core for the specimens. From right to left: original core; intermediate stage, where the core was cut with a sharp box knife; final stage, where the core has been sanded to the shape on the left. The process was quite reliable and repeatable.

Reinforcement material	T300 carbon	E-glass	Kevlar	Dyneema
Energy of baseline (J)	14.9 ± 1.0	39.1 ± 0.8	20.2 ± 0.5	55.5 ± 7.2

Table 3. Energy of baseline specimens for each reinforcement used. Three specimens were tested for each material. Data shown is mean \pm one standard deviation.

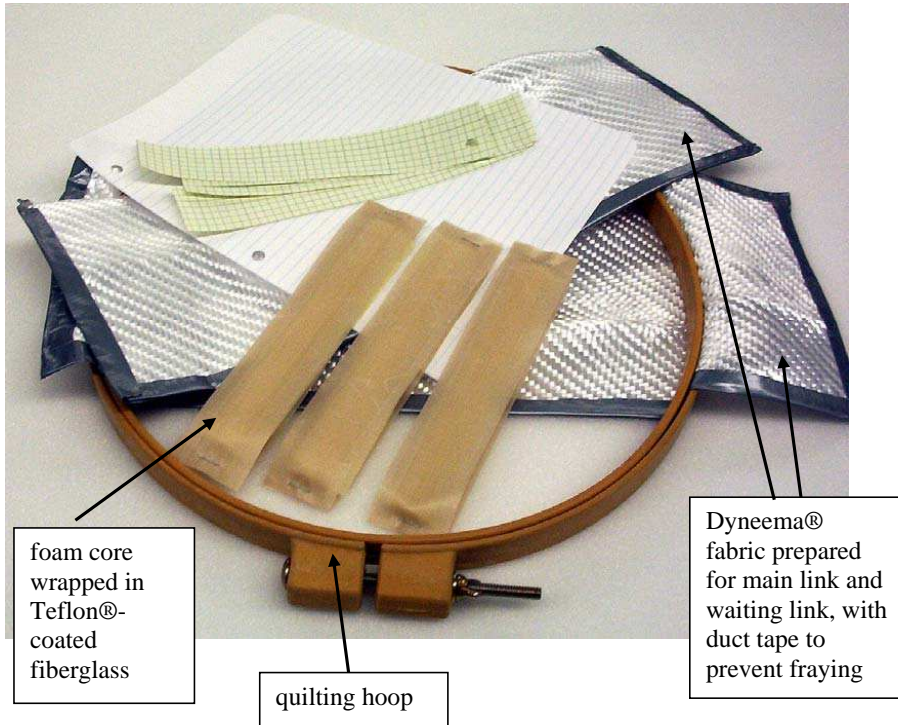


Figure 4. Materials needed to stitch a specimen.



Figure 5. Sewing machine used to stitch, with Kevlar 29 thread, the plies of Dyneema inserted in the quilting hoop, with the aid of engineering paper. This process has also been used for the other materials discussed in the paper.

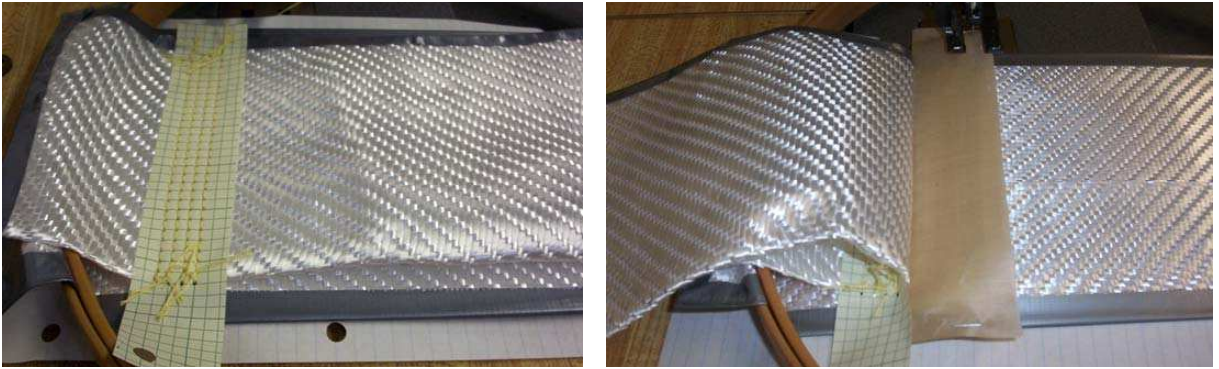


Figure 6. Left: picture of the top layer being folded back to allow the insertion of the wrapped core. Right: stitched Dyneema ready for core insertion.



Figure 7. Dyneema specimen ready for resin infiltration.

are shown in Table 5). The load drop after the main link failure was found to be proportional to the percent wait, so the percent wait was increased. This could lead to higher energy absorption (Figure 10).

Figure 11 shows the load/displacement curve of the carbon specimens with small round core, with and without core, compared to the three baseline specimens. One detects a bistable response of the specimens, but the damaged state is still weaker than the undamaged state; therefore this goal was not met.

However, several additional factors affect the structure's performance, such as the materials' strain and strength, matrix inclusions in the transition area between main link and waiting link, (which led to premature failure), manufacturing-related issues such as the waiting link's alignment, etc. Hence, while the general idea in Figure 10 seems to make sense, it cannot be said a priori that the energy absorption capacity of a bistable structure is proportional to the percent wait for all cases.



Figure 8. Specimen during vacuum-assisted resin transfer molding process (VARTM), after vacuum has been applied and before the specimen is cured in an oven. The red nylon mesh accelerates the infiltration process.



Figure 9. Test of a Dyneema specimen in a 222 kN screw-driven machine. Additional tabbed specimens are visible on the right.

Figure 12 shows side pictures of the fractured specimens in iterations 5–12, Figure 13 documents testing of one specimen and highlights a problem region of excess matrix.

3.1. Discussion on T300 carbon, E-glass and Kevlar specimens. The T300 carbon specimens proved unable to a) survive the strain needed to straighten the waiting link attached to the first failed main link, and b) carry the additional tensile load required to fail the next link in the chain. The average elongation to failure of the three-ply baseline specimens was equal to 1.87%, which is indicative of the strain capability

	<i>Material</i>	<i>Core shape</i>	<i>Percent wait (%)</i>	<i>Energy (J) with / without core</i>
1	T300 carbon	trapezoid	8.8	12.9 / 7.6
2	T300 carbon	small round	5.5	8.2 / 7.3
3	T300 carbon	large round	12	12.3 / 11.5
4	T300 carbon	large round	12	5.8 / 4.5
5	T300 carbon	small round	5.5	4.3 / 4.5
6	T300 carbon	small round	5.5	5.5 / 5.9
7	T300 carbon	large round	12	4.87 / 6.85
8	T300 carbon	round gumdrop	23.4	5.4 / 5.4
9	E-glass	trapezoid	8.8	10.3 / 11.5
10	E-glass	small round	5.5	16.6 / 15.4
11	E-glass	large round	12	11.1 / 4.06
12	E-glass	medium round	9	15.3 / 19.8
13	T300 carbon	medium round	9	5.54 / 6.85
14	Kevlar	small round	5.5	7.48 / –
15	Kevlar	medium round	9	7.76 / –
16	Kevlar	large round	12	8.28 / –
17	Dyneema	small round	5.5	83.9 ± 7.40 / –
18	Dyneema	medium round	9	84.2 ± 3.28 / –
19	Dyneema	large round	12	97.3 ± 12.7 / –
20	Dyneema	very large round	15	114 ± 5.05 / –
21	Dyneema	super-large round	34	133 ± 23.1 / –

Table 4. Results of tensile tests for all configurations.

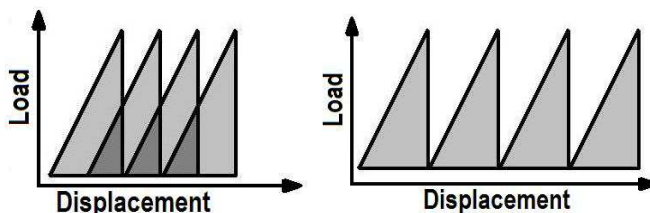


Figure 10. Response of small round core (left) with respect to medium and large core (right). The load drop after the main link breaks is proportional to the percent wait.

Segment Fiber	Energy (percent of baseline value)				
	Small round	Medium round	Large round	Very large round	Super-large round
T-300 carbon	37	37	33	N/A	N/A
E-Glass	42	39	28	N/A	N/A
Kevlar	37	38	41	N/A	N/A
Dyneema	151	152	175	206	240

Table 5. Absorbed energies in terms of baselines, for the round core configurations of T-300 carbon, E-glass, Kevlar and Dyneema. E-glass and Dyneema were the only materials where the damaged state was stronger than the undamaged state (bold numbers). Dyneema was the only material with higher energy absorption than the baseline’s.

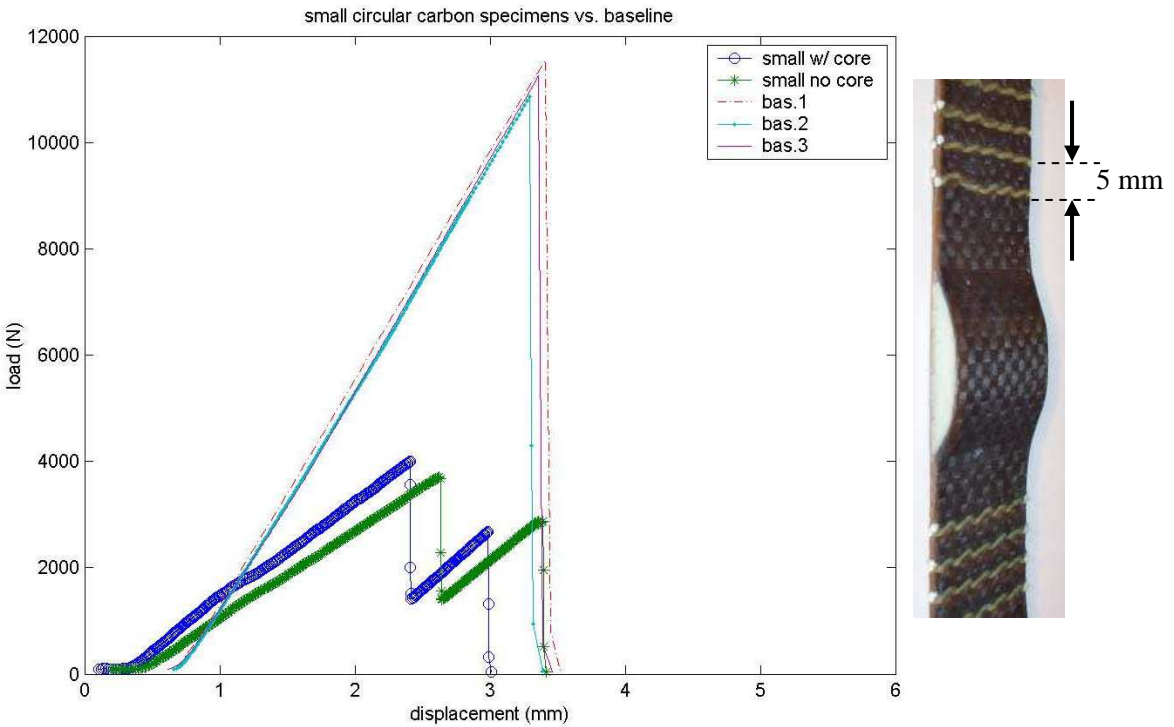
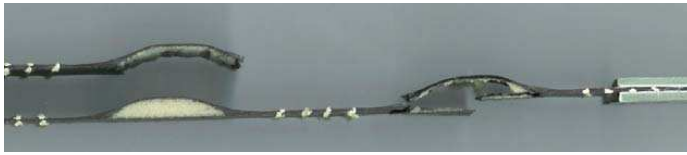


Figure 11. Load/displacement curves of carbon bistable specimens with small round core. One specimen had the core removed (‘no core’). The three baseline curves are shown, as well as a picture of the specimen.

of the chain-like specimens. The response was bistable in some of the specimens, however the damaged state was not stronger than the undamaged state (see Table 5 and Figures 11 and 14).

None of the T300 carbon specimens had the desired behavior. However, experimenting with geometries and use of Teflon-wrapped core was useful, and allowed to identify improved configurations and



Iteration 5, T300 carbon, small circular core, no wrapping of the core. The top specimen had the core removed prior to testing. The response of the two specimens was not bistable.



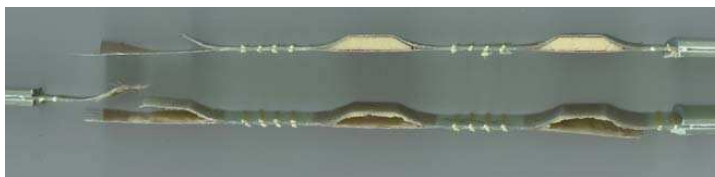
Iteration 6, T300 carbon, small circular core, with core wrapped.



Iteration 7, T300 carbon, large circular core



Iteration 8, T300 carbon, gumdrop core



Iteration 9, E-glass, trapezoid core. The core was removed before the test in the lower specimen.



Iteration 12, E-glass, medium circular core

Figure 12. Side view of specimens shown after fracture. Among these specimens, the only iteration where the response not only was bistable but also has a stronger damaged state, is #12, the E-glass with medium round core. However, in all the cases in this figure, the absorbed energy was considerably less than the baselines’.



Figure 13. Picture of carbon specimen during testing. The matrix inclusion at the intersection of the main and waiting link popped out, causing failure of the specimen.

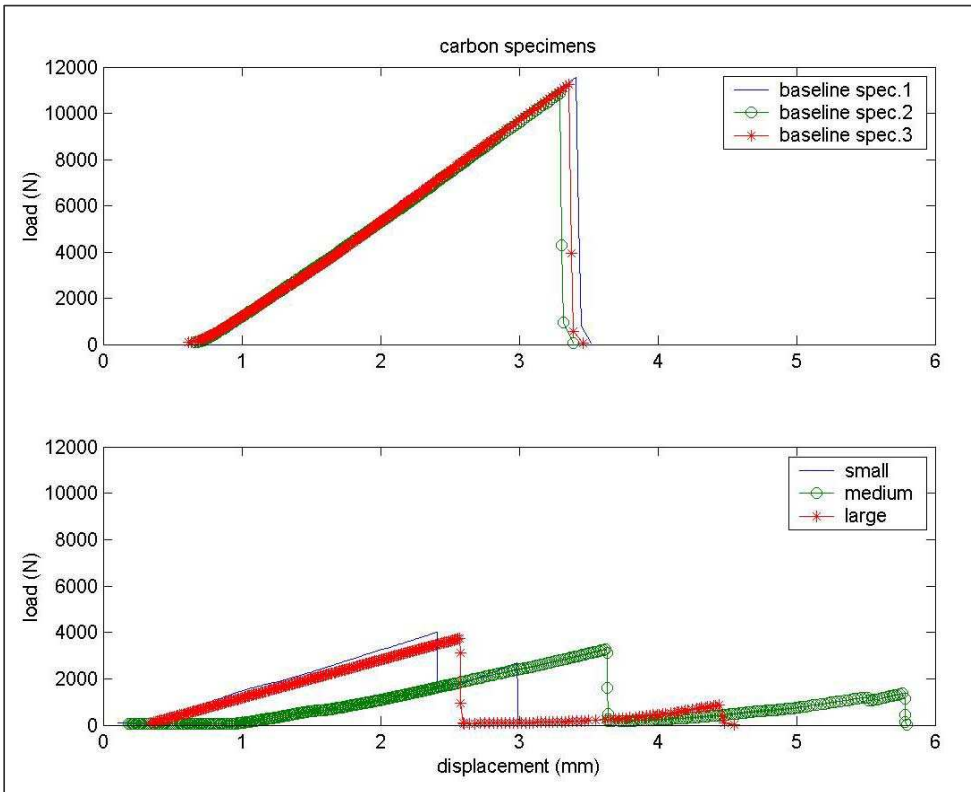


Figure 14. Load/displacement curves for baseline and bistable T300 carbon specimens.

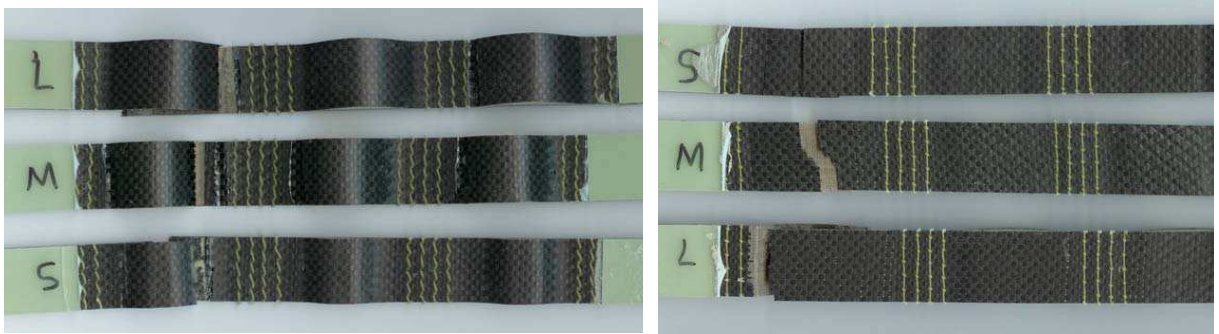


Figure 15. Top and bottom views of fractured main links and waiting links in T300 carbon specimens with small, medium and large round cores. Specimen width is 25.4 mm.

observe and mitigate issues with the curvature of the waiting link: the intersection of main and waiting links tended to be plagued by matrix inclusions which ‘popped out’ during the testing, accelerating failure (note Figure 13). Figure 15 shows bottom and top views of the T300 specimens. Note how the main links failed both near the stitch location and in the center of the link, and the waiting links seem to fail at the concave transition of the waiting link layers.

Three of the four iterations with E-glass specimens showed a bistable response with one of the desired behaviors (damaged state stronger than the undamaged state). The average elongation to failure of the baseline specimens was 3.62%. The much higher elongation to failure of this material with respect to carbon allowed a better performance in terms of bistable behavior, however the specimens did not have enough strength and durability to absorb more energy than their baselines (Figure 16, Table 5). Also, some E-glass specimens suffered from poor alignment of the waiting link material. Figure 17 shows fracture of main and waiting links in E-glass specimens. Similarly to the carbon specimens, fracture of the waiting link, occurs at the intersection of waiting link and main link, but the main link tended to fracture at the stitching.

The Kevlar specimens’ response was similar to the carbon’s. Figures 18 and 19 show the load/displacement curves and the fractured specimens. The average elongation to failure of the baseline was 2.54%.

The primary causes of failure for the T300 carbon, E-glass and Kevlar specimens include

- excessively acute radii in the waiting link,
- damage caused by core removal,
- susceptibility to matrix inclusions next to the core,
- excess matrix at the concave outer surface of the waiting link,
- high shock caused by energy release when the main link fails,
- high shock caused by a nonzero load following fracture,
- tearing due to poorly aligned layers (recall the manual manufacturing process).

3.2. Discussion on Dyneema specimens. Dyneema weave was received after the extensive testing of the previous three reinforcements, and it was the only material capable to absorb more energy than

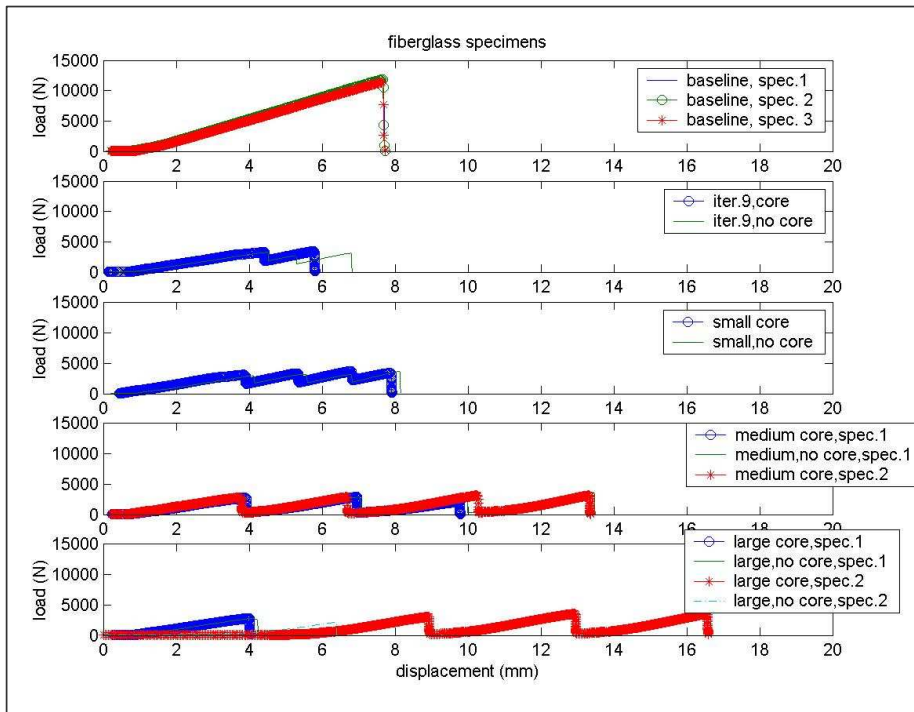


Figure 16. Load/displacement curves for baseline and bistable E-glass specimens.



Figure 17. Top and bottom views of fractured main links and waiting links in E-glass specimens with small, medium and large round cores. Specimen width is 25.4 mm.

its baseline. The average strain of the baseline specimens was 4.7%. Note that the weave had about twice the thickness of the other weaves, but the weight is comparable to that of carbon and E-glass. In most Dyneema specimens, the whole structure was straight and in-plane until the first main link broke. Afterwards, the other main links moved out-of-plane and became somewhat curved. As the waiting link attached to the first fractured main link straightens, it crushes the core, while pushing the main link out of the way. When the last waiting link fails, the structure is still somewhat cohesive.

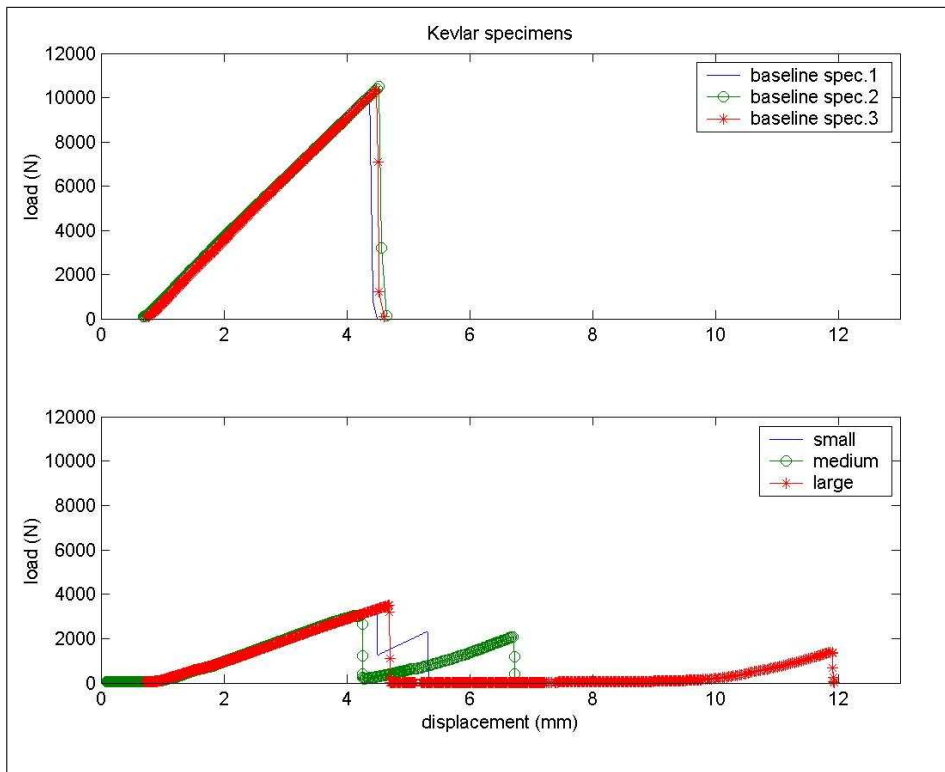


Figure 18. Load/displacement curves for baseline and bistable Kevlar specimens.

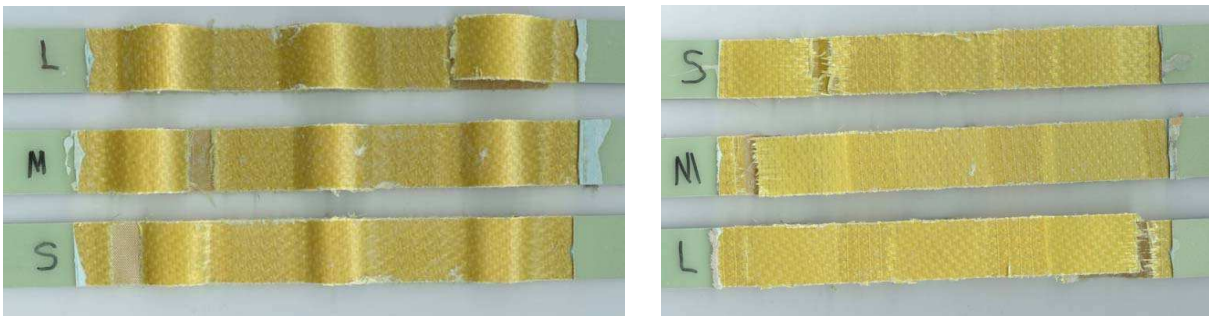


Figure 19. Top and bottom views of fractured main links and waiting links in Kevlar specimens with small, medium and large round cores. Specimen width is 25.4 mm.

The corresponding load/displacement curves show a nonlinear behavior (Figure 20). One of the reasons for the overall increase in absorbed energy is that both elongation to failure and strength are high enough that the waiting links are carrying considerable load by the time a main link fails. Figure 21 shows the lack of a complete fracture in main links and waiting links: different bundles seem to have had progressive failure. Further testing on the Dyneema involved specimens with larger percent waits

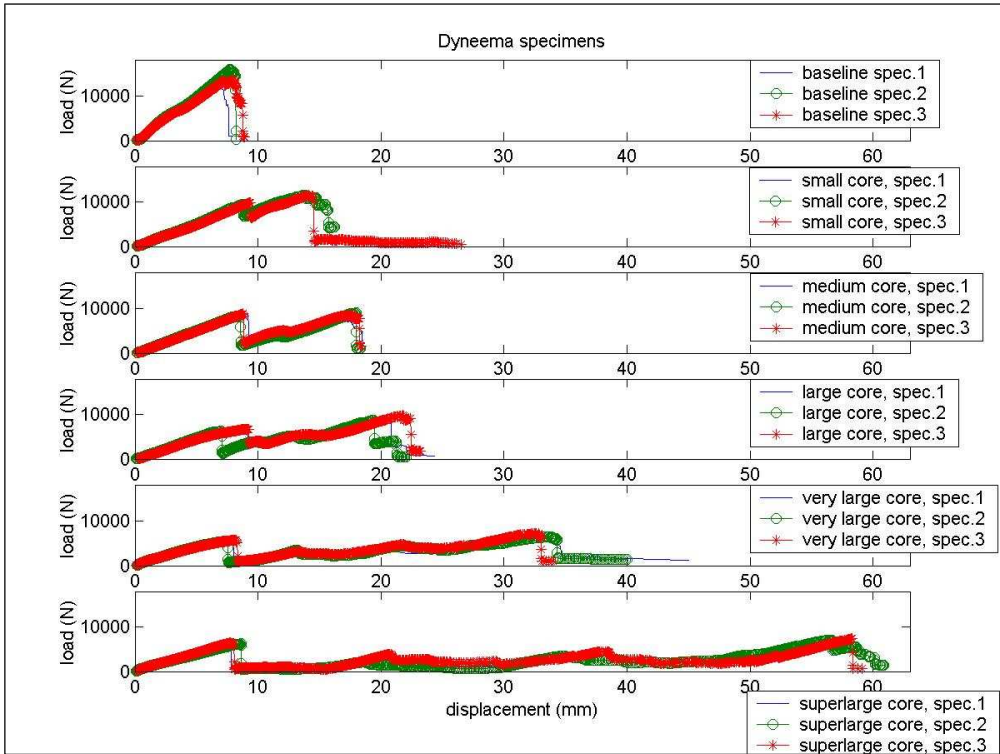


Figure 20. Load/displacement curves for baseline and bistable Dyneema specimens.

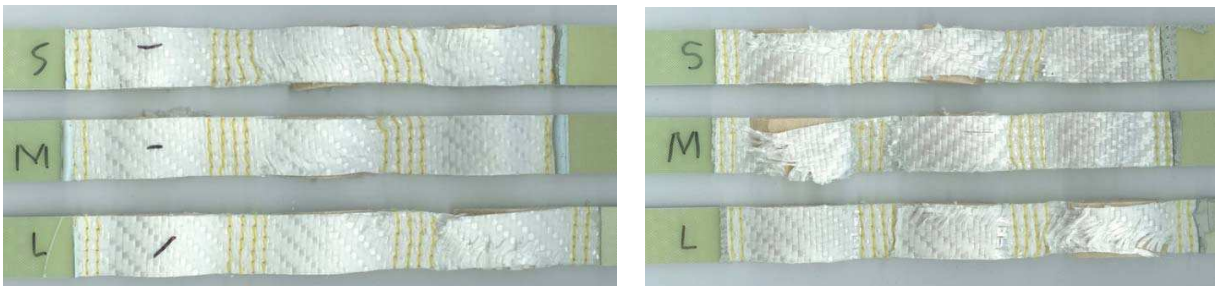


Figure 21. Top and bottom views of fractured main links and waiting links in Dyneema specimens with small, medium and large round cores. Specimen width is 25.4 mm.

(Table 5), and the absorbed energy consistently increased up to 240% of the baseline average energy. (For the nonlinear displacement/load curves of Dyneema, all data up to the point of the last significant load drop are used for the calculation of the energy. Because of that, the end ‘tails’ were not included in this calculation. The other materials’ load/displacement curves are linear and hence the calculation of the energy was straightforward.)

4. Additional observations

Further experiments considered the effect of node composition (i.e. number of stitch rows), element length, and number of elements in a chain. These experiments were carried out on E-glass, the second best material, because the batch of Dyneema had been completely used. Current commercial demands make Dyneema very difficult to obtain for research purposes. However, we hope that it will be possible to complete this study in the future when supplies do come available.

5. Summary and conclusions

This paper discussed the design, manufacturing and testing of composite bistable structures, with the goal of obtaining a) a bistable load/displacement curve which also exhibited a damaged state which higher load carrying capability than the undamaged state, b) higher energy absorption than the traditional laminate-type baselines. Twenty-one different configurations and four materials (T300 carbon, E-glass, Kevlar and Dyneema) were tested in quasistatic tension. Of the four materials, E-glass and Dyneema satisfied the first requirement, but only Dyneema was able to demonstrate a noticeable increase of energy absorption with respect to its baseline. Positive results could be obtained with other configurations of T300 carbon and Kevlar outside those designed in this paper.

This material-based mechanism is very affected by quality of manufacturing, local behavior (i.e. matrix inclusions), elongation to failure, strength, percent weight, node composition, element length. This first study on composite bistable structures under tension shows that they may offer a considerable increase of energy absorption and fail-safe fracture, which could affect the design of composites for all applications where crashworthiness and redundancy are critical aspects of the design.

Acknowledgments

We thank Dr. Andrej Cherkaev and Dr. Elena Cherkaev, Department of Mathematics, University of Utah, for their collaboration, and Dr. Martin Van Es, DSM Corporation, for the donation of Dyneema®.

The work of this paper was performed while Whitman was an M.S. student in the Department of Mechanical Engineering, University of Utah. The experimental work was conducted in the Strength of Materials Lab and in the Composite Manufacturing Lab of that department.

References

- [Cherkaev and Slepyan 1995] A. Cherkaev and L. Slepyan, "Waiting element structures and stability under extension", *Int. J. Damage Mec.* 4:1 (1995), 58–82.
- [Whitman and La Saponara 2007] Z. Whitman and V. La Saponara, "Bistable structures for energy absorption, I: metallic structures under tension", *J. Mech. Mater. Struct.* 2:2 (2007), 347–358.

Received 30 May 2006. Accepted 26 Sep 2006.

ZACHARY WHITMAN: zachary.whitman@swri.org
Southwest Research Institute

VALERIA LA SAPONARA: vlasaponara@ucdavis.edu
Department of Mechanical and Aeronautical Engineering, One Shields Ave, University of California, Davis, CA 95616-5294,
United States

<http://mae.ucdavis.edu/vlasaponara/>